Single-atom sensor for low-frequency electric field

Quan Yuan,[1,2,a)] Shuang-Qing Dai,[2,3,a)] Tai-Hao Cui,[2,3] Pei-Dong Li,[2,3] Yuan-Zhang Dong,[2,3] Zhuo-Zhu Wu,[2,3] Ji Li,[4] Fei Zhou,[2,4] Jian-Qi Zhang,[2] Liang Chen,[2,4] and Mang Feng[2,4,5,6]

[1)] *Guangzhou Institute of Industrial Intelligence, Guangzhou 511458, China*

[2)] *Wuhan Institute of Physics and Mathematics, Innovation Academy of Precision Measurement Science and Technology, Chinese Academy of Sciences, Wuhan 430071, China*

[3)] *University of Chinese Academy of Sciences, Beijing 100049, China*

[4)] *Research Center for Quantum Precision Measurement, Guangzhou Institute of Industry Co., LTD, Guangzhou, 511458, China*

[5)] *Key Laboratory of Low-Dimensional Quantum Structures and Quantum Control of Ministry of Education, Department of Physics and Synergetic Innovation Center for Quantum Effects and Applications, Hunan Normal University, Changsha 410081, China*

[6)] *Department of Physics, Zhejiang Normal University, Jinhua 321004, China*

(*Electronic mail: mangfeng@wipm.ac.cn)

(*Electronic mail: liangchen@wipm.ac.cn)

(*Electronic mail: changjianqi@gmail.com)

Precision measurement of low-frequency electric field (LFEF) signals with frequency from 30 kHz to 300 kHz is crucial for advancing both fundamental science and practical applications, owing to their unique frequency regime. For conventional electromagnetic antennas, the long wavelength (i.e., several kilometers) of the LFEF leads to a severe size constraint that efficient radiation becomes challenging to achieve when the antenna size is much smaller than the long wavelength of the LFEF signals, which in turn results in a reduction of measurement sensitivity and compromises antenna's performance. By exploiting the high intrinsic sensitivity of cold trapped ions to weak alternating electric signals via Coulomb interaction, we demonstrate a single-ion phonon laser sensor acted by an injection-locked $^{40}Ca^{+}$ ion confined in a surface-electrode trap. Combining the beat frequency technique with the injection-locked phonon laser oscillation, we demonstrate a practical and efficient approach for simultaneous extraction of the frequency, phase, and amplitude from a single measurement, without the need for sideband cooling. This approach achieves precision detection for LFEF signals with the sensitivity of 403.8 $\mu V/(m \cdot Hz^{1/2})$ and the detection limit of 61.5 μV/m. Besides, this approach also shows remarkable robustness against noise. Our study helps realizing practical single-atom sensors in the low-frequency regime, opening avenues for applications in subsurface communication, precision metrology, mass spectrometry, and biomedical monitoring.

arXiv:2607.17583v1 [quant-ph] 20 Jul 2026

The precision measurement of weak alternating signals is an important topic in physics and metrology. Such signals often carry critical information about new physical phenomena, ranging from ultralight dark-matter fields[1] and geophysical transients[2] to neuronal oscillations[3]. Their detection is hindered by weak amplitudes, low frequencies, and environmental noise. In particular, precision detection of low-frequency electric fields (LFEFs) between 30 kHz and 300 kHz is of great interest because their long wavelength and low propagation loss are vital for subsurface and underwater wireless communications[4,5]. For conventional antennas, effective coupling to the long wavelength (i.e, several kilometers) of a LFEF requires the antenna size comparable to the signal wavelength, and severe size-wavelength mismatch impairs signal detection capability. The inherent constraint of conventional antennas for LFEFs severely compromises the detection sensitivity of miniaturized antennas, fundamentally hindering the miniaturization of practical LFEF detection systems.

To overcome this difficulty, various measurement techniques have been developed to achieve weak signal detection[6,7], one of which is the beat frequency technique. This technique converts two nearby frequencies into a detectable low-frequency signal, providing a powerful approach for processing optical and electrical signals[8]. It has been extensively applied in optical[9–14], atomic[15–18], and electronic systems[19–22] for communication demodulation[23–25], biomedical signal detection[26–29], and precision measurement[30–32].

In particular, applying the beat frequency technique in laser systems has given rise to various advanced detection techniques, including laser heterodyne detection[33–36], dual-comb spectroscopy[37–40], and fiber Bragg grating[29,41–43]. These techniques represent powerful applications of the beat frequency

[a)] Co-first authors with equal contribution

principle in the optical domain, but not directly applicable to the LFEF detection. Extending the exquisite sensitivity of optical beat frequency techniques to the direct detection of LFEFs remains challenging for conventional photonic systems, primarily due to their susceptibility to environmental noise and limited electro-optic response at these frequencies.

Here, we present a fundamentally distinct LFEF measurement technique for precision detection of electric fields using a trapped ion. As ions are charged and interact with external electric fields via the Coulomb force, they exhibit an high sensitivity to fluctuation of external electric fields due to their extremely high charge-to-mass ratio [44–47]. This intrinsic property allows ion-based electric field sensors to break through the conventional size constraints and be miniaturized down to the micrometer scale with high sensitivity detection for LFEF signals. In our experiment, the trapped ion functions as an injection-locked single-ion phonon laser, the vibrational analog of an optical laser, exhibiting amplification[48] and frequency stabilization via an injection-locking signal[49].

By applying the beat frequency technique to the input LFEF signal and the injection-locked phonon laser, we coherently map the input signal onto the ion's vibration, enabling simultaneous extraction of its frequency, phase, and amplitude in a single measurement. This approach provides high sensitivity and resolution in the kHz regime, while requiring neither sideband cooling nor special operating conditions. It thus offers a compact and practical route to highly sensitive weak-signal sensing.

Our experiment is carried out in a surface-electrode trap (SET) with the measured secular frequency along z-axis of $\omega_z/2\pi = 238.42(0.01)$ kHz. A single $^{40}Ca^{+}$ ion, located at 800 μm above the center of the SET, behaves as a phonon laser in the direction of ω_z under the irradiation of two detuned 397-nm laser beams, where one is red-detuned with Δ_r = -115 MHz and the other is blue-detuned with Δ_b = 30 MHz. We saturate the laser power with the ratio $r = s_b/s_r = 0.58$, where $s_{r(b)}$ represents the saturation parameter of the red (blue)-detuned laser beam. Throughout the whole experiment, an additional over-saturated 866-nm laser beam is always on for repumping. This setup ensures the generation of a stable phonon laser system with the oscillation amplitude of 25.5 μm. In particular, only Doppler cooling of the trapped ions is required in our scheme.

For our purpose, we employ the arbitrary waveform generator (AWG) to apply the injection locking signal $S_i = V_i \sin(2\pi\omega_i t)$ to the axis electrode

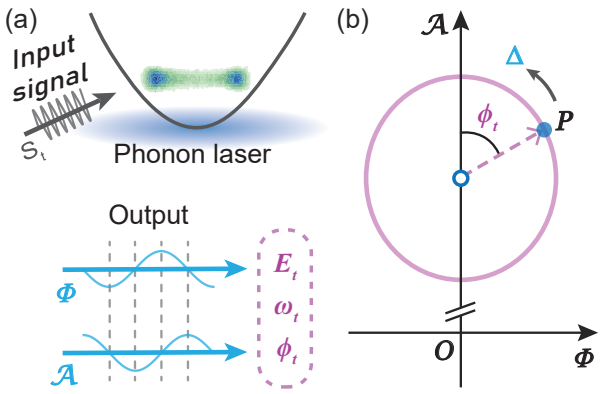

FIG. 1. Principle of the beat frequency measurement by single-ion phonon laser. (a) The scheme of the beat frequency measurement by single-ion phonon laser, where the vibrational motion of the single ion is modulated by the input signal S_t, and the responses are characterized by the evolution of the phase Φ and amplitude $\mathcal{A}$ of the phonon laser. (b) Trajectories in phase-amplitude coordinate of the phonon laser.

of the SET, and inject the synchronization signal into the time-to-amplitude converter[50]. The injection intensity is fixed to be $V_i = 7.5$ mV with the frequency set to be the same as ω_z. As a result, the frequency of the single-ion phonon laser is locked and synchronized with S_i accompanied with an amplified oscillation. The LFEF signal to be detected is also generated from the AWG in the form of $S_t = V_t \sin(2\pi\omega_t t + \phi_t)$ and applied to the axis electrode (see Fig. 1(a)). Thus, the LFEF signal applied to the trapped ion can be denoted as $E_t = kV_t$ with a response parameter k, which is mainly determined by the materials and geometric structure of the axis electrode. We denote the input signal as (V_t, Δ, ϕ_t), where $\Delta = \omega_t - \omega_i$ is the beat frequency between S_i and S_t.

To perform the beat frequency measurement of LFEF signals, we combine two waves of slightly different frequencies, which gives rise to beats at their frequency difference. In our experiment, we utilize the external vibrational motion of the injection-locked phonon laser system to perform beat frequency measurements of LFEF signals. The beat frequency between the injection-locked phonon laser and the input signal S_t generates a modulation of the phonon laser's amplitude and phase. By synchronously monitoring the phonon laser's vibration through photon scattering, we extract the frequency, phase, and amplitude of the input signal S_t from the beat-induced evolution of the phonon laser.

To show the principle in more details, we describe the oscillation displacement of the single-ion phonon laser as $Z = \mathcal{A}\sin(2\pi\omega_i t + \Phi)$, with the slowly vary-

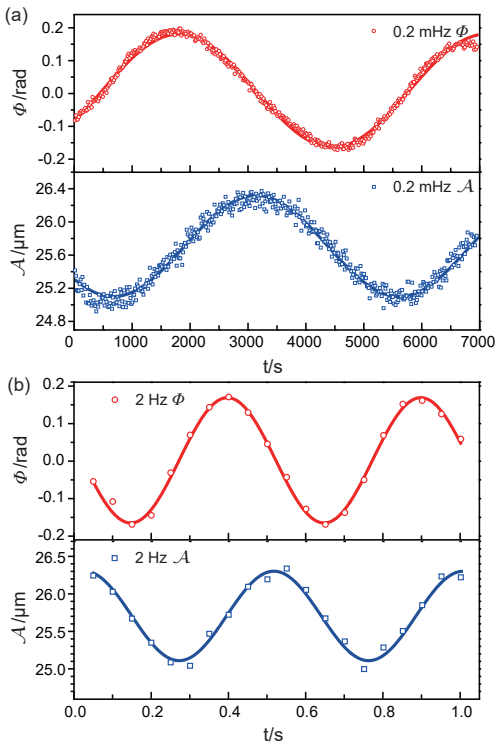

FIG. 2. Beat frequency measurement of sinusoidal input signals. Evolution of the measured phase Φ (red) and amplitude $\mathcal{A}$ (blue) of the phonon laser with input signal of (a) 0.2 mHz and (b) 2 Hz. The red and blue lines are the sinusoidal fitting results of the data points.

ing amplitude $\mathcal{A}$ and phase Φ. We have the motion equation of the ion interacting with two laser beams along the z-axis of the trap, with both S_i and S_t applied,

$$m\ddot{Z} = -m\omega_z^2 Z + F_c + F_g + F(t), \tag{1}$$

where m is the mass of the ion, Z is the displacement of the ion, F_c (F_g) represents the scattering force of the cooling (gain) laser beam, and $F(t) = ke(S_i + S_t) = ke[V_i \sin(2\pi\omega_i t) + V_t \sin(2\pi\omega_t t + \phi_t)]$ corresponds to the force of the applied signals acting on the ion with the response parameter k. A beat frequency emerges from the superposition of the phonon laser and S_t, manifesting as periodic fluctuations on both amplitude and phase of the phonon laser. Here we assume $V_t \ll V_i$ and $|\Delta| \ll \omega_i$ and the outputs of Φ and $\mathcal{A}$ vary periodically with Δ as[50]

$$\Phi \approx -R_p k V_t \sin(\Delta t + \phi_t), \tag{2}$$
$$\mathcal{A} \approx A_0 + R_A k V_t \cos(\Delta t + \phi_t), \tag{3}$$

where the response factors $R_p = e/2m\omega_i\Delta A_0$ and $R_A = e/2m\omega_i\Delta$, with A_0 the average amplitude of the injection-locked phonon laser without the input signal applied.

To illustrate the response of the phonon laser system to the input signal more vividly, we decompose Eqs. (2) and (3) in the phase-amplitude coordinate, as illustrated in Fig. 1(b). Initially the phonon laser lies at the position of $(0, A_0)$, corresponding to the locked phase and the amplified amplitude under the injection locking. After the input signal is applied, the phonon laser is dragged to P along a direction with an angle of ϕ_t to the positive $\mathcal{A}$-axis, and then begins to rotate around $(0, A_0)$ at a frequency of $|\Delta|$ along the elliptical path. A positive (negative) Δ leads to a counterclockwise (clockwise) rotation.

Experimentally, we record the distribution of accumulated photon counts as a function of their arrival time counted by a photomultiplier tube (PMT) and a time-to-amplitude converter. The phase Φ and amplitude $\mathcal{A}$ of the phonon laser can be acquired by fitting the accumulated photon counts with the convolution of the scattering rate of the phonon laser[51,52]. The accumulation time can be set, according to Δ, to meet the sampling theorem. By analyzing the continuously accumulated curves regarding the photon scattering rate, Φ and $\mathcal{A}$ in different moments can be obtained. Then the variations of Φ and $\mathcal{A}$, evolving synchronically with S_t, can be fitted by Eqs. (2) and (3) and thus, we acquire the characteristics of S_t. In our scheme, a higher sampling rate for sinusoidal fitting results in a shorter accumulation time per curve.

Fig. 2 presents the experimentally obtained Φ and $\mathcal{A}$ for (a) $\Delta = 0.2$ mHz and (b) $\Delta = 2$ Hz. These results clearly demonstrate the beat frequency between the phonon laser and the input signal. Moreover, it is evident that both the uncertainties in the measurements and the errors of $\mathcal{A}$ in the fitting curve are significantly higher than those of Φ. This results from the phase locking and limitation of the fluorescence acquisitions. Therefore, in the following experiments, we would fit the measured Φ to Eq. (2) with a sinusoidal function using $\Phi_{fit} = -E_{\rm fit}\sin(\Delta_{\rm fit}t - \phi_{\rm fit})$ to extract the fitting result $E_{\rm fit}, \Delta_{\rm fit}$, and $\phi_{\rm fit}$, where the parameter of the input signal can be derived. However, since the evolution of Φ is the same for both cases of $(V_t, -\Delta, \pi - \phi_t)$ and (V_t, Δ, ϕ_t), we cannot identify the input signal from Φ alone. As such, we use the amplitude $\mathcal{A}$ to provide the necessary discrimination.

By precalibrating how the input signal affects the evolution range of Φ (which will be clarified later in the sensitivity of the amplitude measurement), we can directly convert the fitted amplitude ϕ_{fit} into ϕ_t due to their one-to-one mapping. For example, we fit Eq. (2) with sinusoidal functions to the data in

Fig. 2(a,b) and extract the input signal parameters: (a) (1.26 mV, 0.2 mHz, 0.82π) and (b) (1.20 mV, 2 Hz, -0.11π).

We next discuss the sensitivity and limitations of our protocol for simultaneously detecting the three characteristics of the input signal. Note that the measured frequency difference Δ_{fit} directly reflects the properties of S_t, while the amplitude and phase of the input signal are converted from the measured radian amplitude E_{fit} and phase ϕ_{fit}. We define the sensitivities of frequency, phase and amplitude by the minimum detectable change σ_D, σ_p, and σ_a, i.e., the measurement uncertainties of $\Delta_{fit}, E_{fit}, \phi_{fit}$, within the detection bandwidth $1/\sqrt{t_{tot}}$, as evaluated later from experimental results. Thus they are given by $\eta_D = \sigma_D\sqrt{t_{tot}}$, $\eta_p = \sigma_p\sqrt{t_{tot}}$ and $\eta_a = \sigma_a\sqrt{t_{tot}}/(\partial E_{fit}/\partial E_t)$, respectively, where t_{tot} is the total measurement time.[51,52]

In Table I, we present the results of (1.25 mV, Δ, 0) with Δ varying for a quite wide range from 0.2 mHz to 2 Hz. Obviously, each data point provides a good reconstruction of the input signal with $\Delta_{fit} \approx \Delta$, unequivocally demonstrating the overall reliability of our scheme in this frequency range. With the reduction of Δ, the fitting error (FE), denoting the uncertainty obtained by fitting the measured phase of the phonon laser to sinusoidal function, decreases because more samples are collected over a longer period, while the accuracy also slightly decreases due to the long-term drift of ω_z[50].

By elaborately regulating the electrode voltages of the SET, we can vary Δ to shorten the required total measurement time. Theoretically the phonon laser system can respond to a quite wide range of frequency as long as $|\Delta| \ll \omega_z$ is satisfied. Experimentally, however, our frequency resolution is limited by the sampling rate and system stability. A larger Δ requires less accumulating time, which is unfavorable to the accuracy of the fitting. As for the other hand, a smaller Δ leads to a longer total measurement time for ensuring the fitting accuracy, which requires highly long-term stability of the system. At a frequency near the middle of the range (e.g., Δ = 0.05 Hz) and for t_{tot} = 20 s, σ_D = 0.75 mHz, the optimal frequency sensitivity can be obtained at 3.4 mHz/$\sqrt{\text{Hz}}$.

TABLE I. Comparison of the beat frequency measurements as well as the fitting error (FE) from sinusoidal fitting, where the input signal is set as (1.25 mV, Δ, 0) and total measurement time is $t_{tot} \geq 1/\Delta$ for each data point. For example, we set t_{tot} = 2100 s for Δ = 0.5 mHz, and t_{tot} = 2 s for Δ = 1 Hz.

Δ (Hz)	Δ_{fit} (Hz)	FE (Hz)
2e-4	1.8845e-4	-3.22e-7
3e-4	3.1651e-4	-1.18e-6
5e-4	5.0281e-4	-2.19e-6
1e-3	1.0004e-3	-4.54e-6
2e-3	1.9963e-3	-3.19e-6
5e-3	5.0273e-3	-1.61e-5
0.01	0.0101	-4.16e-5
0.02	0.0204	-1.21e-4
0.05	0.0514	-3.87e-4
0.1	0.1020	-6.06e-4
0.2	0.2033	-2.15e-3
0.5	0.5177	-4.48e-3
1	1.0073	-5.13e-3
2	1.9996	-1.16e-2

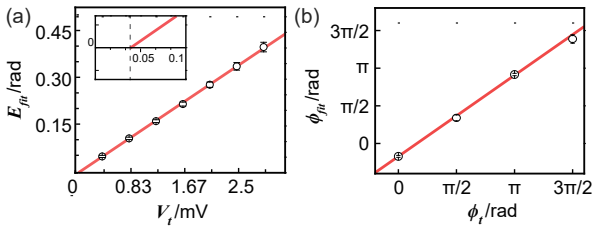

FIG. 3. Evaluation of the accuracy of Φ. (a) The fitting amplitude E_{fit} of Φ versus the given amplitude V_t of the input signal (V_t, 0.05 Hz,0), with V_t varying from 0.42 mV to 2.92 mV. The red line is a linear fit of the data points with the slope of $\partial E_{fit}/\partial V_t$ = 136.8 mrad/mV. (b) The fitting phase ϕ_{fit} of Φ versus the given phase ϕ_t of the input signal (1.25 mV, 0.05 Hz, ϕ_t). Error bars are statistical standard errors from 10 measurements for each data point with t_{tot} = 20 s for each measurement.

The fitting amplitude E_{fit} varies linearly with the given V_t, as plotted in Fig. 3(a). In our experiment, the response parameter k is calculated as 1.3 m^{-1} with the fitted slope of $\partial E_{fit}/\partial V_t$ = 136.8 mrad/mV and $\omega_i/2\pi = \omega_z/2\pi$ = 238.42 kHz. Due to the inherent noises, the fitted line does not pass through the origin but approaches zero at V_t = 46.2 μV, indicating the minimum detectable strength of the LFEF in our system is 61.5 μV/m. Unlike the one-to-one reconstruction in frequency as shown above, the amplitude sensitivity can be improved by increasing the slope $\partial E_{fit}/\partial V_t$. According to Eq. (2), the slope $\partial E_{fit}/\partial V_t$ is inversely correlated with the amplitude of the phonon laser, which is experimentally controlled by the saturation ratio r or the injection intensity V_i[50].

Besides, once V_t increases to a level comparable to V_i, the measured E_{fit} would deviate from the linear fitting and thus reduce the reconstruction accuracy. This deviation may arise from less stable oscillations caused by the competing locking of the input signal and the injection locking signal. Although increasing V_i can broaden the measurement range of V_t that helps promoting accuracy, it favors little for uncertainty reduction[50]. In this case, we have calculated

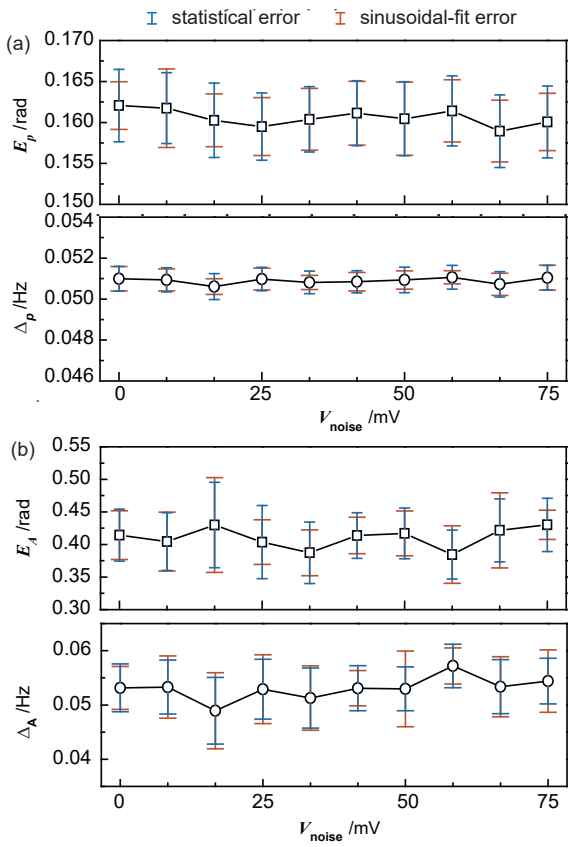

FIG. 4. The influence of different noise amplitudes on the fitted amplitude and frequency obtained via the evolution of the phonon laser's (a) phase and (b) amplitude with an input signal (1.25 mV, 0.05 Hz, 0), where the fitted amplitude/frequency obtained via fitting the evolution of phonon laser's phase and amplitude to Eq. (2) and Eq. (3) respectively are marked as E_p/Δ_p and E_A/Δ_A.Blue error bars are the statistical standard error of 10 measurements, and red error bars are the sinusoidal fitting error.

the amplitude sensitivity to be 403.8 μV/($m\cdot$Hz$^{1/2}$), with $\sigma_a = 9.5$ mrad, which is comparable in order of magnitudes with the amplitude sensitivity of weak electric field signal we have detected in our former work[51].

Similarly, the fitted phase ϕ_{fit} also shows a favorable linear dependence on the given ϕ_t, as plotted in Fig. 3(b), from which we acquire the phase sensitivity of 0.4(0.3) rad/$\sqrt{\text{Hz}}$ with $\sigma_p = 98(65)$ mrad. We notice that the phase has a higher uncertainty than the other two components, because the long-term drift of ω_z mainly impacts the phase shift. This result can be optimized by improving the system stability.

The single-ion phonon laser beat frequency measurement system also demonstrates remarkable robustness against the applied Gaussian white noise. Fig. 4 shows the evolution of the phonon laser's phase and amplitude with the noise increasing from 0 to 75 mV, which is much stronger than the input signal. Neither the fitted amplitudes, E_p, E_A, nor the fitted frequencies, Δ_p, Δ_A, obtained via respectively fitting the evolution of phonon laser's phase and amplitude to Eq. (2) and Eq. (3), show significant correlation with the noise intensity. Notably, both the statistical standard error (blue) and the sinusoidal fitting error (red) don't increase significantly with the noise amplitude, contrary to expectations. While the increased noise induces a measurable decrease in phonon laser amplitude, the measured phase stability remains exceptionally high[50]. Our approach is robust against noises since the noises predominantly affect the amplitude of a harmonic oscillator rather than the phase. This phase stability arises from injection locking to the phonon laser, which locks the oscillation frequency to the injection locking signal and thereby suppresses phase fluctuations. Crucially, parameters derived from sinusoidal fitting exhibit no significant correlation with the noise intensity, and the associated errors do not increase as expected. This unexpected noise immunity highlights the method's potential for high-precision measurements in complex, noisy environments.

We have experimentally demonstrated a practical and efficient scheme for measuring LFEF signals using an injection-locked single-ion phonon laser combined with the beat frequency technique, achieving a minimum detectable strength of LFEF of 61.5 μV/m, which is comparable in order of magnitudes to former trapped-ion electric-field sensing experiments[49,51,52]. Besides, different from our former work in electric field signal detection[47], in the present work we directly apply the input LFEF signal to electrode without modulation, and realize the extraction of amplitude, frequency, and phase of the input signal in a single measurement. The sensitivity of our scheme is determined by the measurement signal-to-noise ratio of the phonon laser, as well as the stability of the phonon laser's amplitude and phase. These quantities can be directly improved by enhancing the fluorescence collection efficiency and the long-term stability of the system, which could be realized through a more compact trap design and reduced secular frequency drift[53,54]. In addition, enhancing the long-term stability of the system enables long-time continuous measurement, thereby further improving the frequency resolution.

Our approach enables the simultaneous extraction of the complete characteristics of the LFEF signal (i.e., amplitude, frequency, and phase) in a single

measurement, making it more efficient than conventional counterparts. Moreover, our protocol operates near the secular frequency of the SET, which can be adjusted from 90 kHz to 300 kHz and can be expanded from a few kHz to the MHz regime in other types of ion traps[55,56]. Notably, this technique works without sideband cooling and relies entirely on sensitive optical detection. As a result, it is practical and easily applicable in trapped-ion systems for accurately detecting LFEF signals in noisy environments. Finally, the phase sensitivity of our scheme opens exciting possibilities for designing high-resolution mass spectrometry[57,58] and detecting biochemical oscillations[59].

Our study advances the development of LFEF sensors and inspires advancements in frequency modulation and conversion in nano-scale systems. Beyond trapped ions, the demonstrated transduction mechanism can be applied to other platforms, for example, the optomechanical microcavities[60,61], electromechanical resonators[62], and optical tweezers[63], as well as to broader applications, such as long-wave communication[64], industrial and medical inspection[65], and meteorological monitoring[66].

Acknowledgements

This work was supported by National Natural Science Foundation of China under Grant Nos. U25D9005, 12534020, 12304315, 12074346, 12074390, 12074280, 92265107, by Science and Technology Projects in Guangzhou under Grant Nos. 202201011727 and 2023A04J0050, by Guangdong Provincial Quantum Science Strategic Initiative under Grand No. GDZX2305004 and No. GDZX2505001, by Nansha Senior Leading Talent Team Technology Project under Grant No. 2021CXTD02, by Science and Technology Project of SGCC 52120025005C-338-WLCY, and by the Special Project for Research and Development in Key Areas of Guangdong Province under Grant No. 2020B0303300001.

[1] O. Tretiak, X. Zhang, N. L. Figueroa, D. Antypas, A. Brogna, A. Banerjee, G. Perez, and D. Budker, "Improved bounds on ultralight scalar dark matter in the radio-frequency range," Physical review letters **129**, 031301 (2022).

[2] M. Li, J. Lu, M. Parrot, H. Tan, Y. Chang, X. Zhang, and Y. Wang, "Review of unprecedented ulf electromagnetic anomalous emissions possibly related to the wenchuan m s= 8.0 earthquake, on 12 may 2008," Natural Hazards and Earth System Sciences **13**, 279–286 (2013).

[3] G. Buzsaki and A. Draguhn, "Neuronal oscillations in cortical networks," science **304**, 1926–1929 (2004).

[4] D. Latypov, "Compact quantum vlf/elf sources for submarine to air communication," in *2022 Sixth Underwater Communications and Networking Conference (UComms)* (2022) pp. 1–4.

[5] S.-U. Yoon, L. Cheng, E. Ghazanfari, Z. Wang, X. Zhang, S. Pamukcu, and M. T. Suleiman, "Subsurface monitoring using low frequency wireless signal networks," in *2012 IEEE International Conference on Pervasive Computing and Communications Workshops* (2012) pp. 443–446.

[6] H. V. Poor, *An introduction to signal detection and estimation* (Springer Science & Business Media, 2013).

[7] M. Huang, A. Zhou, L. Wang, Y. Wang, and G. Qiu, "Review of weak signals detection methods," in *2023 IEEE 16th International Conference on Electronic Measurement & Instruments (ICEMI)* (IEEE, 2023) pp. 98–104.

[8] E. D. Diebold, B. W. Buckley, D. R. Gossett, and B. Jalali, "Digitally synthesized beat frequency multiplexing for submillisecond fluorescence microscopy," Nature Photonics **7**, 806–810 (2013).

[9] R. Kompfner, "Optical communications," Science **150**, 149–155 (1965).

[10] M. J. French, J. C. Angus, and A. G. Walton, "Laser beat frequency spectroscopy," Science **163**, 345–351 (1969).

[11] A. D. Ludlow, M. M. Boyd, J. Ye, E. Peik, and P. O. Schmidt, "Optical atomic clocks," Rev. Mod. Phys. **87**, 637–701 (2015).

[12] P. Zemánek and J. Lazar, "Use of the beat frequency between two modes for frequency stabilization of internal-mirror lasers," Appl. Opt. **33**, 6333–6339 (1994).

[13] C. Greiner, B. Boggs, T. Wang, and T. W. Mossberg, "Laser frequency stabilization by means of optical self-heterodyne beat-frequency control," Opt. Lett. **23**, 1280–1282 (1998).

[14] D. Burghoff, T.-Y. Kao, N. Han, C. W. I. Chan, X. Cai, Y. Yang, D. J. Hayton, J.-R. Gao, J. L. Reno, and Q. Hu, "Terahertz laser frequency combs," Nature Photonics **8**, 462–467 (2014).

[15] D. Allan, "Statistics of atomic frequency standards," Proceedings of the IEEE **54**, 221–230 (1966).

[16] M. Jing, Y. Hu, J. Ma, H. Zhang, L. Zhang, L. Xiao, and S. Jia, "Atomic superheterodyne receiver based on microwave-dressed rydberg spectroscopy," Nature Physics **16**, 911–915 (2020).

[17] M. Cai, Z. Xu, S. You, and H. Liu, "Sensitivity improvement and determination of rydberg atom-based microwave sensor," Photonics **9** (2022), 10.3390/photonics9040250.

[18] K. Dixon, K. Nickerson, D. W. Booth, and J. P. Shaffer, "Rydberg-atom-based electrometry using a self-heterodyne frequency-comb readout and preparation scheme," Phys. Rev. Appl. **19**, 034078 (2023).

[19] S. Neemat, O. Krasnov, and A. Yarovoy, "An interference mitigation technique for fmcw radar using beat-frequencies interpolation in the stft domain," IEEE Transactions on Microwave Theory and Techniques **67**, 1207–1220 (2019).

[20] S. Scherr, S. Ayhan, B. Fischbach, A. Bhutani, M. Pauli, and T. Zwick, "An efficient frequency and phase estimation algorithm with crb performance for fmcw radar applications," IEEE Transactions on Instrumentation and Measurement **64**, 1868–1875 (2015).

[21] R. Wang, C. Hu, X. Fu, T. Long, and T. Zeng, "Micro-doppler measurement of insect wing-beat frequencies with w-band coherent radar," Scientific reports **7**, 1396 (2017).

[22] G. S. Kulkarni, K. Reddy, Z. Zhong, and X. Fan, "Graphene nanoelectronic heterodyne sensor for rapid and sensitive vapour detection," Nature Communications **5**, 4376 (2014).

[23] M. Jing, Y. Hu, J. Ma, H. Zhang, L. Zhang, L. Xiao, and S. Jia, "Atomic superheterodyne receiver based on microwave-dressed Rydberg spectroscopy," Nature Physics **16**, 911–915 (2020).

[24] R. F. Lucy, K. Lang, C. J. Peters, and K. Duval, "Optical

superheterodyne receiver," Appl. Opt. **6**, 1333–1342 (1967).
[25]A. Mirzaei, H. Darabi, and D. Murphy, "A low-power process-scalable super-heterodyne receiver with integrated high-q filters," IEEE Journal of Solid-State Circuits **46**, 2920–2932 (2011).
[26]I. Salmeen, D. Gill, L. Rimai, J. McCormick, V. Maher, W. Arnold, and M. Hight, "Application of laser beat frequency spectroscopy to the detection and characterization of an oncogenic rna virus," Biochemical and Biophysical Research Communications **47**, 1172–1178 (1972).
[27]Y. Zhang, Y.-N. Tan, T. Guo, and B.-O. Guan, "Beat frequency trimming of dual-polarization fiber grating lasers for multiplexed sensor applications," Opt. Express **19**, 218–223 (2011).
[28]Y. Guo, X. Tong, Y. Shen, and H. Wu, "Wearable optical fiber beat frequency digital sensing system for real-time non-invasive multiple human physiological parameters monitoring," Journal of Lightwave Technology **41**, 2911–2920 (2023).
[29]D. Lo Presti, C. Massaroni, C. S. Jorge Leitão, M. De Fátima Domingues, M. Sypabekova, D. Barrera, I. Floris, L. Massari, C. M. Oddo, S. Sales, I. I. Iordachita, D. Tosi, and E. Schena, "Fiber bragg gratings for medical applications and future challenges: A review," IEEE Access **8**, 156863–156888 (2020).
[30]Y. Dai, Q. Sun, S. Tan, J. Wo, J. Zhang, and D. Liu, "Highly sensitive liquid-level sensor based on dual-wavelength double-ring fiber laser assisted by beat frequency interrogation," Opt. Express **20**, 27367–27376 (2012).
[31]L. Gao, L. Huang, L. Chen, and X. Chen, "Study on fiber ring laser in sensing application with beat frequency demodulation," Optics & Laser Technology **45**, 137–141 (2013).
[32]E. D. Diebold, B. W. Buckley, D. R. Gossett, and B. Jalali, "Digitally synthesized beat frequency multiplexing for sub-millisecond fluorescence microscopy," Nature Photonics **7**, 806–810 (2013).
[33]V. V. Protopopov, *Laser heterodyning*, Vol. 149 (Springer, 2009).
[34]M. Jin, S.-J. Tang, J.-H. Chen, X.-C. Yu, H. Shu, Y. Tao, A. K. Chen, Q. Gong, X. Wang, and Y.-F. Xiao, "1/f-noise-free optical sensing with an integrated heterodyne interferometer," Nature Communications **12**, 1973 (2021).
[35]Y. Liang, W. Fu, Q. Li, X. Chen, H. Sun, L. Wang, L. Jin, W. Huang, and B.-O. Guan, "Optical-resolution functional gastrointestinal photoacoustic endoscopy based on optical heterodyne detection of ultrasound," Nature Communications **13**, 7604 (2022).
[36]A. Cygan, S. Wójtewicz, H. Jóźwiak, G. Kowzan, N. Stolarczyk, K. Bielska, P. Wcisło, R. Ciuryło, and D. Lisak, "Dispersive heterodyne cavity ring-down spectroscopy exploiting eigenmode frequencies for high-fidelity measurements," Science Advances **11**, eadp8556 (2025).
[37]I. Coddington, N. Newbury, and W. Swann, "Dual-comb spectroscopy," Optica **3**, 414–426 (2016).
[38]B. Bernhardt, A. Ozawa, P. Jacquet, M. Jacquey, Y. Kobayashi, T. Udem, R. Holzwarth, G. Guelachvili, T. W. Hänsch, and N. Picqué, "Cavity-enhanced dual-comb spectroscopy," Nature Photonics **4**, 55–57 (2010).
[39]G. Millot, S. Pitois, M. Yan, T. Hovhannisyan, A. Bendahmane, T. W. Hänsch, and N. Picqué, "Frequency-agile dual-comb spectroscopy," Nature Photonics **10**, 27–30 (2016).
[40]D. I. Herman, M. Walsh, M. K. Kreider, N. Lordi, E. J. Tsao, A. J. Lind, M. Heyrich, J. Combes, J. Genest, and S. A. Diddams, "Squeezed dual-comb spectroscopy," Science **387**, 653–658 (2025).
[41]A. Othonos, "Fiber bragg gratings," Review of Scientific Instruments **68**, 4309–4341 (1997).
[42]K. Hill and G. Meltz, "Fiber bragg grating technology fundamentals and overview," Journal of Lightwave Technology **15**, 1263–1276 (1997).
[43]Y. Guo, Y. Shen, X. Tong, and H. Wu, "Simultaneous measurement of vibration and temperature based on fbg and dbr fiber laser beat frequency digital sensing system," Optical Fiber Technology **75**, 103155 (2023).
[44]M. Brownnutt, M. Kumph, P. Rabl, and R. Blatt, "Ion-trap measurements of electric-field noise near surfaces," Rev. Mod. Phys. **87**, 1419–1482 (2015).
[45]C. L. Degen, F. Reinhard, and P. Cappellaro, "Quantum sensing," Rev. Mod. Phys. **89**, 035002 (2017).
[46]N. P. de Leon, K. M. Itoh, D. Kim, K. K. Mehta, T. E. Northup, H. Paik, B. S. Palmer, N. Samarth, S. Sangtawesin, and D. W. Steuerman, "Materials challenges and opportunities for quantum computing hardware," Science **372**, eabb2823 (2021).
[47]Y.-Q. Wei, Q. Yuan, L. Chen, T.-H. Cui, J. Li, S.-Q. Dai, F. Zhou, and M. Feng, "Time and frequency resolution of alternating electric signals via single-atom sensor," Phys. Rev. Appl. **19**, 064062 (2023).
[48]K. Vahala, M. Herrmann, S. Knünz, V. Batteiger, G. Saathoff, T. W. Hänsch, and Th. Udem, "A phonon laser," Nature Physics **5**, 682–686 (2009).
[49]S. Knünz, M. Herrmann, V. Batteiger, G. Saathoff, T. W. Hänsch, K. Vahala, and Th. Udem, "Injection Locking of a Trapped-Ion Phonon Laser," Physical Review Letters **105**, 013004 (2010).
[50]"See our supplementary materials for details.".
[51]Z. Liu, Y. Wei, L. Chen, J. Li, S. Dai, F. Zhou, and M. Feng, "Phonon-Laser Ultrasensitive Force Sensor," Physical Review Applied **16**, 044007 (2021).
[52]Y.-Q. Wei, Y.-Z. Wang, Z.-C. Liu, T.-H. Cui, L. Chen, J. Li, S.-Q. Dai, F. Zhou, and M. Feng, "Detection of DC electric forces with zeptonewton sensitivity by single-ion phonon laser," Science China Physics, Mechanics & Astronomy **65**, 110313 (2022).
[53]K. G. Johnson, J. D. Wong-Campos, A. Restelli, K. A. Landsman, B. Neyenhuis, J. Mizrahi, and C. Monroe, "Active stabilization of ion trap radiofrequency potentials," Rev. Sci. Instrum. **87**, 053110 (2016).
[54]D. T. C. Allcock, L. Guidoni, T. P. Harty, C. J. Ballance, M. G. Blain, A. M. Steane, and D. M. Lucas, "Reduction of heating rate in a microfabricated ion trap by pulsed-laser cleaning," New Journal of Physics **13**, 123023 (2011).
[55]Z. D. Romaszko, S. Hong, M. Siegele, R. K. Puddy, F. R. Lebrun-Gallagher, S. Weidt, and W. K. Hensinger, "Engineering of microfabricated ion traps and integration of advanced on-chip features," Nature Reviews Physics **2**, 285–299 (2020).
[56]S. Xu, X. Xia, Q. Yu, A. Parakh, S. Khan, E. Megidish, B. You, B. Hemmerling, A. Jayich, K. Beck, J. Biener, and H. Häffner, "3d-printed micro ion trap technology for quantum information applications," Nature **645**, 362–368 (2025).
[57]E. Deslignière, V. C. Yin, E. H. T. M. Ebberink, A. D. Rolland, A. Barendregt, T. P. Wörner, K. O. Nagornov, A. N. Kozhinov, K. L. Fort, Y. O. Tsybin, A. A. Makarov, and A. J. R. Heck, "Ultralong transients enhance sensitivity and resolution in Orbitrap-based single-ion mass spectrometry," Nature Methods **21**, 619–622 (2024).
[58]F.-H. Chen, C.-Y. Cheng, S.-W. Chou, C.-H. Yang, I.-C. Lu, and M.-L. Yeh, "High-Resolution Intact Protein Analysis via Phase-Modulated, Stepwise Frequency Scan Ion Trap Mass Spectrometry," Analytical Chemistry **96**, 14867–14876 (2024).
[59]C. Fei, Y. Cao, Q. Ouyang, and Y. Tu, "Design principles

for enhancing phase sensitivity and suppressing phase fluctuations simultaneously in biochemical oscillatory systems," Nature Communications **9**, 1434 (2018).

[60] T. Kuang, R. Huang, W. Xiong, Y. Zuo, X. Han, F. Nori, C.-W. Qiu, H. Luo, H. Jing, and G. Xiao, "Nonlinear multifrequency phonon lasers with active levitated optomechanics," Nature Physics **19**, 414–419 (2023).

[61] Q. Zhang, C. Yang, J. Sheng, and H. Wu, "Dissipative coupling-induced phonon lasing," Proceedings of the National Academy of Sciences **119**, e2207543119 (2022).

[62] Y. Wen, N. Ares, F. J. Schupp, T. Pei, G. A. D. Briggs, and E. A. Laird, "A coherent nanomechanical oscillator driven by single-electron tunnelling," Nature Physics **16**, 75–82 (2020).

[63] R. M. Pettit, W. Ge, P. Kumar, D. R. Luntz-Martin, J. T. Schultz, L. P. Neukirch, M. Bhattacharya, and A. N. Vamivakas, "An optical tweezer phonon laser," Nature Photonics **13**, 402–405 (2019).

[64] Z. Qu and M. Lai, "A Review on Electromagnetic, Acoustic, and New Emerging Technologies for Submarine Communication," IEEE Access **12**, 12110–12125 (2024).

[65] P. Gajšek, P. Ravazzani, J. Grellier, T. Samaras, J. Bakos, and G. Thuróczy, "Review of Studies Concerning Electromagnetic Field (EMF) Exposure Assessment in Europe: Low Frequency Fields (50 Hz–100 kHz)," International Journal of Environmental Research and Public Health **13**, 875 (2016).

[66] F. Ahmadi, I. V. McLoughlin, S. Chauhan, and G. ter-Haar, "Bio-effects and safety of low-intensity, low-frequency ultrasonic exposure," Progress in Biophysics and Molecular Biology **108**, 119–138 (2012).